

A new unified approach for modeling hot rolling of steel Part 1: Comparison of models for recrystallization

J. Orend^{a,b}, F. Hagemann^b, F. Klose^b, B. Maas^b, H. Palkowski^{a,*}

^aInstitute for Metallurgy, Robert-Koch-Straße 42, 38678 Clausthal, Germany

^bSalzgitter Mannesmann Forschung GmbH, Eisenhüttenstraße 99, 38239 Salzgitter, Germany

Abstract

Models for the microstructure evolution during hot rolling are reviewed. The basic macroscopic phenomena related to recrystallization are summarized. Constitutive models based on semi empirical equations are compared to more sophisticated models based on cellular automata, vertex and Monte-Carlo-Potts methods. The applicability of each kind of model approach for online and offline process control in steel industry is discussed. While constitutive models are still state-of-the-art for online process control, mesoscale models with a spatial representation of the microstructure can provide better predictive capabilities at the cost of long computation times. To fill this gap a new approach based on modeling the interaction of an ensemble of multiple grains is outlined and first simulation results are presented. The proposed approach allows the unified modeling of dynamic, static and metadynamic recrystallization as well as grain growth.

Keywords: Recrystallization, Model, Simulation, Process Control, Grain Growth, Hot Rolling, Microstructure

1. Introduction

The microstructure evolution during hot rolling is of great interest for the industrial production of steel and has therefore been subject of research in the past decades. Recrystallization during and after rolling is one of the mechanisms that can be used for grain refinement [1]. The resulting microstructure after rolling is also important for the following phase transformation during cooling having a significant influence on the mechanical properties of hot rolled products. In consequence, controlling the recrystallization is one opportunity for controlling the mechanical properties and in turn gives room for saving expensive alloying elements. Therefore models with good predictive capabilities are necessary.

Since dynamic recrystallization had been observed by Greenwood and Worner [2], many theories and models for the description of recrystallization during and after deformation have been developed. These models differ in terms of complexity, characteristic length scale, practical usability and the considered materials. Some of them have been reviewed by Senuma et al. [3], Militzer [4] and more recently by Hallberg [5] and Xiao et al. [6].

Additionally the usability of the different model types for technical applications, like process control or numerical simulations of hot forming processes, is discussed. One important aspect is the required experimental effort necessary for determining material parameters. Constitutive models use a large number

of empirical parameters whereas models with long computation times are not applicable for inverse analysis methods which are often necessary for parameter identification in an industrial context. Therefore a new approach that combines benefits from constitutive and more sophisticated physical models is proposed.

2. Phenomena related to recrystallization

Several phenomena on macroscopic and microscopic scale can be related to recrystallization. Some of them are summarized below.

- During deformation recrystallization can occur after exceeding a critical strain referred to as dynamic recrystallization (*DRX*) [7]. In figure 1 flow curves from cylindrical hot compression tests with 42CrMo4 steel are shown. For strains larger than the peak strain a decrease of the flow stress can be observed that is considered to be caused by *DRX*.
- At high strain rates the flow stress monotonously tends to a lower steady state stress after reaching the peak stress. For lower strain rates a damped oscillation of the flow stress can be observed instead what is referred to as cyclic recrystallization [7].
- The strain ε_p at the peak stress increases with strain rate and decreases with temperature [7].
- The criteria for the transition from continuous to cyclic recrystallization resulting in grain coarsening depends on the Zener-Holomon-parameter and the initial grain size [8].

*Corresponding author

Email addresses: jan.orend@tu-clausthal.de (J. Orend), f.hagemann@sz.szmf.de (F. Hagemann), f.klose@sz.szmf.de (F. Klose), b.maas@sz.szmf.de (B. Maas), heinz.palkowski@tu-clausthal.de (H. Palkowski)

- The grain size during deformation in the steady state regime correlates with the steady state stress as shown by Sakai et al. [1].
- Recrystallization after deformation is called static recrystallization (*SRX*). If *DRX* has occurred during deformation the recrystallization kinetics strongly depends on the strain rate of the previous deformation. This case is often referred to as metadynamic recrystallization (*MDRX*).
- After rapid changes of strain rate or temperature during deformation the flow stress settles on a new steady state value. Before steady state is reached transient oscillations can be observed [1, 9, 10].
- If *DRX* is completed, the austenite grain size after deformation depends on temperature. In figure 2 this is shown for two specimens of 42CrMo4 that have been deformed to the logarithmic strain $\varepsilon = 0.8$ with a strain rate of 5 s^{-1} at temperatures of $900 \text{ }^\circ\text{C}$ and $1000 \text{ }^\circ\text{C}$. The specimens have been quenched directly after deformation.

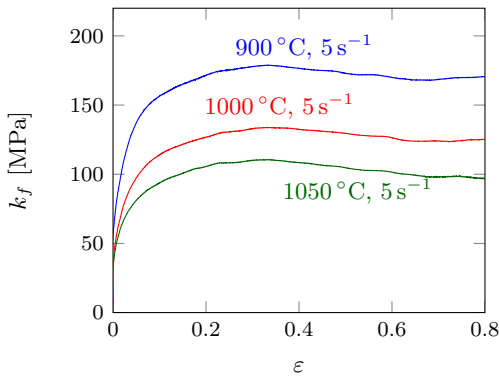


Figure 1: Flow stress curves at different temperatures measured in cylindrical hot compression tests of 42CrMo4 steel samples. After exceeding a specific plastic strain the flow stress decreases due to dynamic recrystallization.

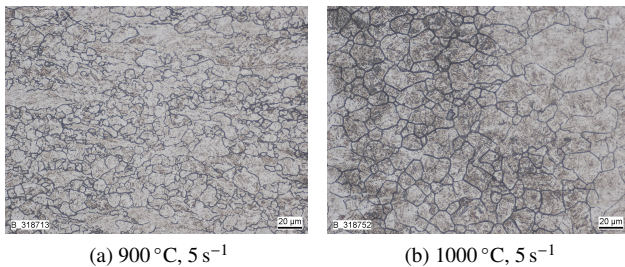


Figure 2: Revealed prior austenite grain boundaries after hot deformation and quenching of 42CrMo4 to $\varepsilon = 0.5$ with a strain rate of $\dot{\varepsilon} = 5 \text{ s}^{-1}$.

3. Models for recrystallization

One way to model the microstructure evolution is to model the observed phenomena summarized above with a set of suitable mathematical functions as proposed by Sellars and Whiteman [11]. These functions include several material parameters that are derived from experimental data. Another way is to model the physical mechanism like work hardening, grain boundary movement and nucleation of new grains that lead to the observed phenomena. To do so it is necessary to have some kind of representation of the state of the microstructure. This can be a set of scalar variables, a set of distribution functions or a spatial representation of the microstructure. Such models are described in subsection 3.2 and 3.3. In this paper we focus on model approaches that play a major role in the development of microstructure models for practical applications. Machine learning techniques like artificial neural networks and fuzzy logic can be used for the prediction of the microstructure [12–14]. However, these methodologies provide “Black-Box” models that do not allow for an insight view of the processes and are therefore not discussed in this paper.

In the following major approaches for modeling recrystallization are described. At the end of each section the features and constraints of each model are pointed out.

3.1. Constitutive models

Constitutive models provide a simple way of describing the microstructure evolution mostly by closed form equation, which makes it possible to use them even in simple spread sheet applications.

3.1.1. Classical models for process control applications

Sellars and Whiteman [11] proposed a constitutive model designed for the application of the simulation of the microstructure evolution during hot rolling that built the starting point for many other models developed by several groups [15–20, 3, 21]. In this paper we only want to give a brief outline of the basic concept behind this type of model. It has to be noted that a multitude of modified or extended versions of the empirical submodels below exist in literature. As input parameter these models use temperature T , strain ε and strain rate $\dot{\varepsilon}$ of each deformation step, the initial average grain size d_0 and the time t after the prior deformation. The output parameters are the recrystallized volume fraction X and the average grain size d . Constitutive microstructure evolution models distinguish between different recrystallization phenomena (*DRX*, *MDRX*, *SRX* and grain growth) that are modeled separately. Each model contains material parameters to be derived from experiments. The recrystallized volume fraction and the prior austenite grain size have to be determined after thermomechanical treatments under various processing conditions, to allow for the determination of material parameters by inverse analysis methods. Many models use the parameter

$$Z = \dot{\varepsilon} \exp\left(\frac{Q_{\text{def}}}{RT}\right) \quad (1)$$

introduced by Zener and Hollomon [22] with Q_{def} as an activation energy and $R = 8.314 \frac{\text{J}}{\text{molK}}$ as the universal gas constant

to combine the dependency of strain rate $\dot{\varepsilon}$ and temperature T into one parameter. The activation energy can be determined with the method proposed by [23]. The recrystallized volume fraction is often described by a modified version of the JOHNSON-MEHL-AVRAMI-KOLMOGOROV equation [24]. For SRX it can be written as

$$X = 1 - \exp\left(-0.693\left(\frac{t}{t_{0.5}}\right)^n\right) \quad (2)$$

with $t_{0.5}$ being the time elapsed until the volume has recrystallized. The time $t_{0.5}$ is calculated with an empirical equation of the common form

$$t_{0.5} = A_{SRX} \varepsilon^{p_{SRX}} d_0^q Z^{r_{SRX}} \exp\left(\frac{Q_{SRX}}{RT}\right) \quad (3)$$

with n , A_{SRX} , p_{SRX} , q , r_{SRX} and Q_{SRX} as material parameters and d_0 as the average grain size prior to the previous deformation. The equation can also be extended to take the effect of niobium into account as proposed by Hodgson and Gibbs [25]. The average diameter of the recrystallized grains is then calculated with

$$d_{SRX} = \varepsilon^{p_d} d_0^{q_d} \exp\left(\frac{Q_D}{RT}\right) \quad (4)$$

where p_d , q_d and Q_D are material parameters.

The onset of DRX during deformation is described by a critical strain

$$\varepsilon_c = A_c d_0^{p_c} Z^{n_c} \quad (5)$$

that has to be exceeded with A_c , p_c and n_c as material parameter. For the volume fraction recrystallized by DRX the time is replaced by strain resulting in

$$X_{DRX} = 1 - \exp\left[B\left(\frac{\varepsilon - \varepsilon_c}{\varepsilon_X}\right)^k\right] \quad (6)$$

with ε_X being the strain at which the volume fraction X has been recrystallized. The strain ε_X can be described by an empirical equation of the same form as equation 5. B and k are material constants. The grain size of the recrystallized grains can be calculated using

$$d_{DRX} = CZ^r \quad (7)$$

where r and C are material parameters. If DRX has occurred the kinetics of recrystallization after deformation depends on the strain rate, i.e. metadynamic recrystallization. The time $t_{0.5}$ decreases with increasing strain rate [25]. Taking this effect into account Hodgson and Gibbs give $t_{0.5,MD}$ as

$$t_{0.5,MD} = k_{MD} Z^{n_{MD}} \exp\left(\frac{Q_{MD}}{RT}\right) \quad (8)$$

with k_{MD} , n_{MD} and Q_{MD} as material parameters [25]. The recrystallized grain size by $MDRX$ can be calculated with an equation of the form of equation 7 with an extra set of material parameters for $MDRX$ (C_{MDRX} , r_{MDRX}). For multistage deformation the effect of work hardening of the previous deformations and of recrystallization on the dislocation density has to be taken into account. To do so the concept of accumulated strain is used by many authors [15, 18, 25]. The strain of each pass is

accumulated to ε_{ACC} . This accumulated strain is decreased depending on the recrystallized volume fraction X resulting in an effective strain $\varepsilon_{eff,i}$ that can be used for the calculation of the flow stress. For the calculation of $\varepsilon_{eff,i}$ various approaches have been discussed by Hodgson and Gibbs [25]. One of them is a linear law of mixtures as

$$\varepsilon_{eff,i} = \varepsilon_i + \lambda(1 - X) \varepsilon_{i-1} \quad (9)$$

with $\lambda = 1$ for C-Mn steels.

Since only average values are considered it is not possible to track multiple volume fractions that have been recrystallized at different time steps. The large number of material parameters make such models easily adjustable to experimental data but also makes them demanding on the scope of the experiments. Although such models cannot describe the influence of the previous processing path due to the lack of inner state variables, they show good agreement with experimental results at steady state conditions, whereas cyclic recrystallization and transient oscillations cannot be described.

3.1.2. Luton and Sellars model for cyclic recrystallization

While the models above aim for practical applications the following model was a starting point for later models considering cyclic recrystallization. Observing DRX during hot torsion tests with nickel and nickel-iron alloys Luton and Sellars [7] propose a model that describes the transition from cyclic to steady state behavior. They assumed that DRX is initiated after exceeding a critical strain ε_c and introduced a strain ε_X to characterize the strain related to the time t_X needed for a large fraction X to recrystallize under constant strain rate conditions. If $\varepsilon_X < \varepsilon_c$ they suppose cyclic recrystallization and otherwise continuous recrystallization behavior.

They calculate the recrystallized volume fraction X with

$$X = 1 - \exp(-kt^n) \quad (10)$$

where t is the time after initiation of DRX and k and n are constants.

The flow stress is calculated as superposition of the flow stress $\sigma_e(\varepsilon)$ and $\sigma_i(\varepsilon)$ for each time increment i . The function $\sigma_e(\varepsilon)$ describes the flow stress without recrystallization at the considered constant temperature and strain rate. For each time increment i a new function $\sigma_i(\varepsilon) = \sigma_e(\varepsilon - \varepsilon_i)$ is introduced. The flow stress is then given as a superposition by

$$\sigma = \sum_0^i X_i \sigma_i + \left(1 - \sum_0^i X_i\right) \sigma_e \quad (11)$$

where X_i is the volume fraction that has been recrystallized in the increment i .

This model is able to describe the transition from periodic to continuous recrystallization. However, it does not describe the damping of the oscillation for cyclic recrystallization.

3.2. Inner state variable models

Since microstructure evolution depends on the current microstructure, models using inner state variables have been in-

roduced. In this section some early model approaches are discussed that were also the basis for more recent models using spatial representations of the microstructure.

3.2.1. Stüwe and Ortner

Stüwe and Ortner [26] suggest a model for *DRX* that describes the recrystallized volume fraction and the resulting flow stress during deformation depending on strain rate and temperature based on the evolution of the dislocation density. In this model the average dislocation density can be seen as an inner state variable. They calculate the flow stress σ with

$$\sigma = AGb\sqrt{\bar{\rho}} \quad (12)$$

with b as the length of the burgers vector, G as shear modulus, $\bar{\rho}$ as average dislocation density and A as a material parameter.

The increase of the dislocation density during deformation due to work hardening is

$$\frac{\partial \rho}{\partial \varepsilon} = \frac{2(l+c)}{lcb} \quad (13)$$

where l and c are the dimensions of the area swept by one dislocation loop of the burgers vector b . In contrast to Luton and Sellars [7] Stüwe and Ortner [26] assume that *DRX* starts after the time

$$t = t_0 = \frac{\rho_n}{\dot{\rho}} \quad (14)$$

for a constant $\dot{\rho}$ after a critical dislocation density ρ_n has been exceeded instead of using a critical strain criterion. For spherical growth with a constant grain boundary velocity v_n the recrystallized volume fraction X after the time t_n is given by

$$X = \left(\frac{v_n(t_n - t_0)}{R} \right)^3 \quad (15)$$

where R is the traveling distance and for the given assumptions the radius of the recrystallized grains. It has to be noted that v_n depends on the grain boundary mobility that is a function of the temperature. The average dislocation density $\bar{\rho}$ needed for the calculation of the flow stress by equation 12 is determined by integrating over the radius of the grains with

$$\bar{\rho} = \frac{3}{4\pi R^3} \int_0^R \rho(r) 4\pi r^2 dr \quad (16)$$

to take into account that the volume behind a moving boundary has a very low dislocation density producing a gradient of ρ from the inner to the outer region of the grain.

While the model can describe a transition from single peak to multiple peak behavior for the combination of low strain rates and high temperatures, the theoretical stress strain curves published by Stüwe and Ortner show a saw like shape that has not been observed in experiments. In contrast to the constitutive models described above recrystallization and the calculation of flow stress are combined into one model. The model also relies on the assumption of constant strain rate and temperature. Hence the model does not include the evolution of the grain size, its effect on nucleation rate and grain boundary movement are not considered. This issue has been addressed with the model developed by Sandström and Lagneborg described below.

3.2.2. Sandström and Lagneborg

In response to the models by Luton and Sellars and Stüwe and Ortner, Sandström and Lagneborg [27] point out, that the current grain size should also be taken into account. They proposed a new model that describes the evolution of the dislocation density distribution. They distinguish between the dislocation density in the subgrain walls ρ_d and the homogeneous dislocation density between the subgrain walls ρ . The volume distribution of both kinds of dislocations are described by the functions $g(\rho, t)$ and $G(\rho_d, t)$ with

$$\int g(\rho, t) d\rho = 1 \quad (17)$$

$$\int G(\rho_d, t) d\rho_d = 1. \quad (18)$$

The time derivative of ρ is given by

$$\frac{d\rho}{dt} = \frac{\dot{\varepsilon}}{bl} - 2M\tau\rho^2 \quad (19)$$

considering work hardening and recovery. Here l is the mean free path of the dislocation and M the dislocation mobility. Recovery for the dislocations in the subgrain walls is neglected so that their evolution is given by

$$\frac{d\rho_d}{dt} = \frac{\dot{\varepsilon}}{bl_d} \quad (20)$$

where the mean free path l_d is directly related to the subgrain size. They conclude, that l has to be much larger than l_d if the main part of the dislocations are accumulated in the subgrain walls which is reported by Stüwe and Ortner [26] to be also necessary for the calculation of realistic values of the flow stress. According to equation 20 the relation between the critical strain ε_{cr} and the critical dislocation density ρ_{cr} for the onset of recrystallization is given as

$$\varepsilon_{cr} = bl_d\rho_{cr}. \quad (21)$$

The time derivative of the recrystallized volume fraction is given by

$$\frac{dX}{dt} = \int_{\rho_{cr}}^{\infty} \frac{\xi\gamma_D}{D} v(\rho_d) G(\rho_d, t) d\rho_d \quad (22)$$

where D is the grain diameter and ξ a constant given as $\xi = 3$. The velocity of the grain boundary $v(\rho)$ is given by

$$v(\rho) = m\tau\rho \quad (23)$$

with the grain boundary mobility m and τ as dislocation line energy. The parameter γ_D is called mobile fraction and describes the effect that some of the grain boundaries do not move. In the model of Sandström and Lagneborg γ_D is assumed to be constant.

The average stress is assumed to depend on the dislocation density in the subgrains and is also calculated using equation 12 but with the average dislocation density being

$$\bar{\rho} = \int_{\rho_0}^{\rho_s} \rho g(\rho, t) d\rho \quad (24)$$

where

$$\rho_s = \sqrt{\frac{\dot{\epsilon}}{2blM\tau}} \quad (25)$$

is the dislocation density when work hardening and recovery are in balance. While the dislocation density is described by distribution functions the grain size is only represented by an average grain diameter D . The evolution of D is described as

$$\frac{dD}{dt} = m \frac{\gamma}{D} - D \frac{dX}{dt} \ln N(D) \quad (26)$$

with the grain boundary mobility m , the grain boundary energy γ and the amount of grains N nucleated per parent grain after one recrystallization cycle.

Like the model by Stöwe and Ortner the model proposed by Sandström and Lagneborg [28] describes the recrystallization combined with the evolution of the dislocation density. Additionally it also considers the evolution of the average grain size. It is able to describe the damped oscillations in flow curves at low strain rates. In comparison with data from experiments with nickel the calculated peak strain at high strain rates is too high. This is explained by not taking into account the strain rate dependency of the mean free path l and the dislocation mobility m .

3.3. Models with spatial representation

Instead of describing the microstructure only with average values some more sophisticated models use a 2D or 3D spatial representation of the microstructure. This representation then evolves according to a set of certain rules that represent the physical mechanisms. The common principle here is the minimization of the free energy. For this there are various methodologies that are not only used for modeling recrystallization but for a broad range of applications. As for the models above temperature and strain rate are the input parameters but here both parameters can change with time. These models output a virtual representation of the grain morphology and the dislocation density that can be used for the calculation of the flow stress.

3.3.1. Cellular Automata

The Cellular Automata (CA) method is based on the work of Ulam [29] and Von Neumann [30]. A CA consists of a set of cells that are commonly ordered in a lattice. Each cell has a state described by a set of variables and is related to a defined set of cells that are called neighborhood. The transition of one state to another is defined by a set of rules that is applied at each evolution step. These rules can only rely on the state of one cell and its neighborhood at the previous evolution step. Starting with Hesselbarth and Göbel [31] many groups have developed models for recrystallization utilizing the CA method [32–40].

In particular Kugler and Turk [41] used a two-dimensional CA with a rectangular grid for the simulation of multistage deformations. To use the CA to describe a virtual microstructure the state of one cell consists of four variables including one variable for the dislocation density ρ_i and the crystal orientation. The

evolution of the dislocation density is calculated by integration of

$$\frac{\partial \rho_i}{\partial \gamma} = k_1 \sqrt{\rho_i} - k_2 \rho_i \quad (27)$$

for each cell where γ is the shear strain, k_1 a hardening coefficient and k_2 a strain rate and temperature depend parameter describing recovery. The flow stress is calculated with equation 12 using

$$\bar{\rho} = \frac{1}{n} \sum_{i=1}^n \rho_i \quad (28)$$

where n is the number of cells. Adjacent cells with the same orientation belong to the same grain. At the grain boundary the transition from one orientation to another occurs depending on the grain boundary velocity calculated by

$$v = m \Delta f \quad (29)$$

with Δf as the driving force per unit area that is a function of the difference of the dislocation densities and the grain boundary energy. The grain boundary mobility m is given by

$$m = \frac{b\delta D}{k_B T} \exp\left(\frac{Q_b}{RT}\right) \quad (30)$$

taking the characteristic grain boundary thickness δ and the boundary self-diffusion coefficient D into account. R is the universal gas constant, k_B is the Boltzmann constant and Q_b is an activation energy. New grains are created at the grain boundary if a critical dislocation density ρ_{cr} is exceeded with a probability

$$P = k \dot{\epsilon} \exp\left(-\frac{\omega}{T}\right) \Delta t \quad (31)$$

where k and ω are material parameters and Δt the time increment of one simulation step.

Kugler and Turk show that their model is able to describe the transition from continuous to cyclic softening at a constant temperature with decreasing strain rate and for constant strain rate with increasing temperature. They also performed numerical experiments with two deformation stages for the analysis of the simulated post deformation recrystallization. They found that exceeding a certain transition strain during the first deformation results in a transition from weak to strong strain rate dependency of the recrystallization kinetics. It can be concluded that a model of this kind can describe the transition from *SRX* to *MDRX* without introducing submodels or special case handling for each recrystallization process as it is necessary for the constitutive models described earlier.

3.3.2. Monte Carlo Potts method

The application of the Monte Carlo Potts algorithm for modeling grain growth and recrystallization started with the work of Sahni et al. [42]. Similar to CA models a lattice is used as representation of the microstructure. Each of the cells, also called Monte Carlo Units (MCU), has a state Q that indicates the misorientation and the affiliation of the cell to one specific grain. Neighboring cells with different values of Q define a

grain boundary. A basic algorithm for the simulation of grain growth has been described by Zöllner and Streitenberger [43]. A random *MCU* with the current state Q_x is temporarily set to a state Q_y with $Q_y \neq Q_x$. The difference of the energy ΔE between the states Q_x and Q_y is then calculated by a Hamiltonian H that depends on the possible misorientation between the cell and its neighbor cells. The resulting energy difference ΔE is used to calculate a probability

$$p = \begin{cases} m, & \Delta E \leq 0 \\ m \exp\left(\frac{-\Delta E}{k_B T}\right), & \Delta E > 0 \end{cases} \quad (32)$$

with k_B as Boltzmann constant and m as grain boundary mobility for the transition from the state Q_x to Q_y . During one Monte Carlo step one of these reorientation attempts is performed for each cell.

Hence this approach mimics the principle of least actions it can be used to model the grain boundary movement without the definition of specific evaluation rules, but to the cost of additional computation time compared to *CA* models.

3.3.3. Vertex models

Vertex models also use a spatial description of the microstructure. In contrast to *CA* models these models do not use a lattice. Instead, the shape of the grains is only described by a set of geometrical features like the vertices illustrated in figure 3. This reduces the needed amount of memory and allows the simulation of larger grain ensembles compared to the *CA* method. The initialization is often done by a Voronoi tessellation, sometimes followed by a simulated annealing [44, 45], that can be performed with the Lloyd-algorithm [46].

Nagai et al. [47] use a mesh with vertices at the triple points of the grain boundaries in the 2D case. The grain boundaries were modeled by straight lines connecting the vertices. They introduced a force attached to the triple points resulting from the energy minimization by optimizing the angles between the grain boundaries. This model has been extended by several authors to allow curved boundaries. Weygand et al. [45] insert additional vertices that divide the lines or planes representing the grain boundary into multiple segments. Cocks and Gill [44, 48] use cubic splines for modeling curved boundaries in the two dimensional case. They also show that the variational principle can be applied to derive equations for the velocity of the vertices to model curvature-driven grain growth. Telley et al. [49] and Schüle [50] utilize the Laguerre tessellation, a Voronoi tessellation with radical weighting, for the simulation of grain growth so only the coordinates of the center and the weighting are needed to describe one grain.

While the utilization of the vertex approach for the simulation of grain growth is common, models are very rare that also consider nucleation. Hence only the geometry of the grain boundaries is described this approach does not provide a spatial dislocation density in the interior of the grains like models based on the *CA* approach or the Monte Carlo Potts method. For modeling nucleation the dislocation density has to be stored in an additional data structure.

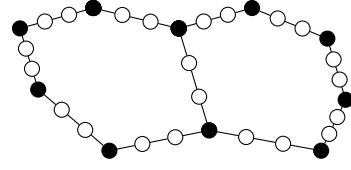


Figure 3: Illustration of two grains in a simple 2D vertex model. Additionally to the vertices (filled) at the triple points each grain boundary line is divided into segments by virtual vertices.

4. Ensemble model

In the following the new model is outlined combining features of more physical based approaches like *CA* models mentioned above with short computation times needed for process control applications. A more detailed description of this model will follow in the second part of this publication.

4.1. Outline of a new approach

The processes involved in recrystallization are time dependent and influence each other as outlined in figure 4. In the model strain rate $\dot{\epsilon}$ and temperature T are the input parameters. Instead of using a spatial representation of the microstructure or

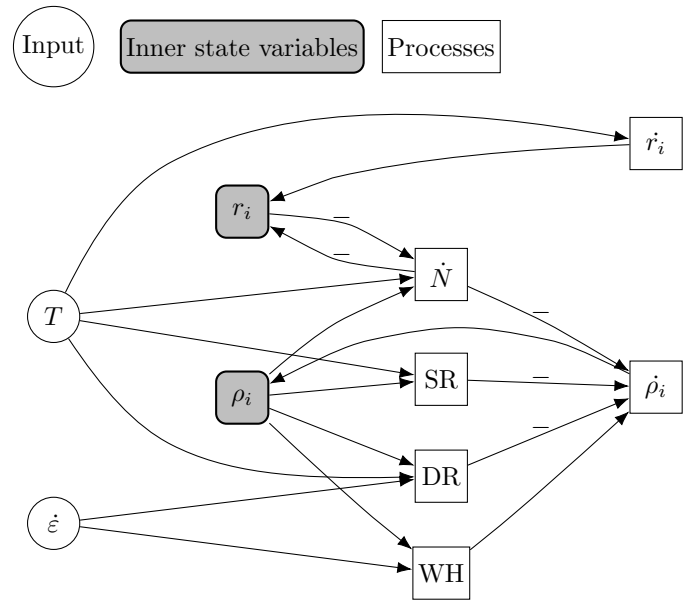


Figure 4: Graph of the processes considered for the new model to be involved in *DRX* and their dependencies. The arrows indicate the direction of an influence. Arrows labeled with (-) indicate a decrease of the influenced quantity. Strain rate $\dot{\epsilon}$ and temperature T are the input parameters. The state is defined by a generalized variable r_i describing the size and the dislocation density ρ_i of each grain. The state is changed by the processes of work hardening (WH), dynamic recovery (DR) and static Recovery (SR) effecting the time derivative of the dislocation density $\dot{\rho}_i$ and by nucleation of new grains (\dot{N}) and grain growth (\dot{r}_i).

average values, the microstructure is described as an ensemble of

grains. Similar to a cell in a CA model each grain i has state variables like the average dislocation density ρ_i and a generalized variable r_i describing the grain size. These can be evolved by the processes of nucleation of new grains (\dot{N} in figure 4), grain growth (\dot{r}_i), dynamic recovery (DR), static recovery (SR) and work hardening (WH). WH and SR are considered by the use of equation 27 for the time derivative of the dislocation density $\dot{\rho}$. Each grain has its own constant shape represented by a ratio

$$\frac{V(r_i)}{S(r_i)} = \kappa_i r_i \quad (33)$$

between grain volume $V(r_i)$ and surface $S(r_i)$ with κ_i as a geometric constant that has to be set at the initialization of the simulation. The ensemble consists of grains in a specified volume that has to be kept constant. During the simulation the size r_i of each grain is adjusted by the integration of \dot{r}_i to reduce the free energy of the system in terms of grain boundary energy and energy stored by dislocations in the volume of the grain. During the grain boundary movement the power

$$\dot{W}_{\text{Diss}} = \frac{1}{2m} \dot{r}_i^2 S(r_i) \quad (34)$$

is dissipated with m as grain boundary mobility. The time derivative of r_i is given by

$$\dot{r}_i = m \left(-3\kappa_i (\tau\rho_i + \lambda) - \frac{2}{r_i} \gamma \right) \quad (35)$$

where τ is the dislocation line energy, γ the grain boundary energy per unit area and λ a Lagrange multiplier. Similar to the approach chosen by Kugler and Turk [41] new grains are generated with a temperature dependent probability if a critical dislocation density ρ_{cr} is exceeded. Preliminary simulation results of this model are discussed below.

4.2. Simulation results

In order to investigate the dynamic behavior of the model simulations under transient conditions were carried out. In figure 5 the results from a simulated deformation at a temperature of 1000°C with a rapid change of the strain rate from 5 s^{-1} to 1 s^{-1} at $\varepsilon = 0.5$ are shown. The flow stress first increases until it reaches a maximum at ε_p . During the first deformation stage a decrease of the average grain size can be observed starting at a strain ε_c that is much smaller than ε_p . After the strain rate change to the smaller strain rate a transient oscillation of the average grain diameter and the flow stress can be observed. This behavior has also been observed in simulations with a CA model by Kroc [33] and in experiments by Sakai and Jonas [8] and Frommert [9].

To illustrate the dependency on strain rate and temperature the average grain size after a deformation step is shown in figure 6. For the combination of low strain rate and high temperature the model predicts grain coarsening. In this case the nucleation rate is relatively low in relation to the growth rate of the grains. At high strain rates $\dot{\varepsilon} > 20\text{ s}^{-1}$ the available time for recrystallization decreases, so at low temperatures the grain size remains at the initial state. At higher temperatures where

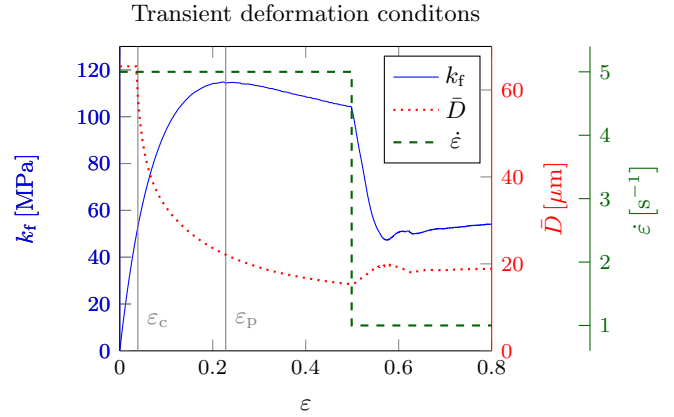


Figure 5: Results from simulated deformation under transient conditions. The calculated flow stress at a temperature $T = 1000^\circ\text{C}$ for an initial average grain diameter $d_0 = 70\text{ }\mu\text{m}$ is shown. At the strain $\varepsilon = 0.5$ the strain rate is changed from 5 s^{-1} to 1 s^{-1} . Following transient oscillation average grain size and flow stress settle on new steady state values.

recrystallization is faster there is still grain refinement. The minimum of the grain size is at the lowest temperature in a strain rate regime where DRX is completed and the strain rate is high enough to induce a high nucleation rate by a high work hardening rate.

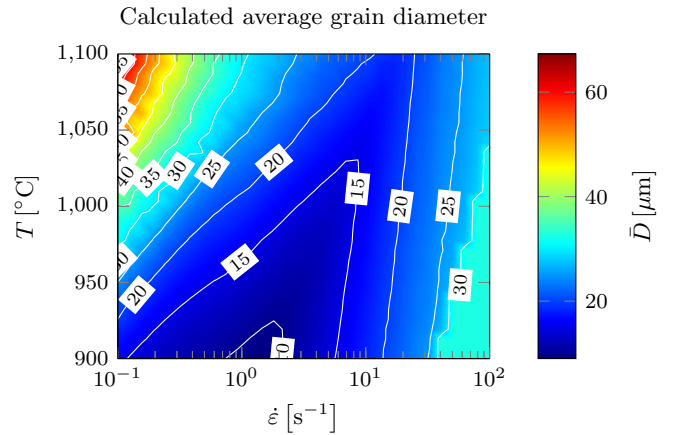


Figure 6: Grain size map for one simulated deformation. For a deformation with $\varepsilon = 0.5$ and an initial grain diameter of $d_0 = 35\text{ }\mu\text{m}$ the calculated average value of the grain diameter immediately after deformation for different strain rates and temperatures is shown. For the combination of low strain rates and high temperatures the model predicts grain coarsening, at high strain rates recrystallization is not completed.

5. Discussion

The models described above diverge in their underlying assumptions and modeling techniques. The major features and

constraints are summarized in figure 7. For the use of microstructure evolution models in technical applications, like forming simulations or process control, a minimum of computational effort is preferred. Constitutive models for the recrystallization during hot deformation as described in subsection 3.1 support fast calculations of average values describing the microstructure like grain diameter or recrystallized volume fraction. Due to their simplicity and low computation times these kinds of models are popular for process control applications. However, there are some drawbacks for the practical application that give motivation for the development of models that include more knowledge about the physical processes.

Constitutive models describe the microstructure evolution in a phenomenological way, so each phenomenon like flow stress, *DRX*, *SRX*, *MDRX* and grain growth are described individually by empirical submodels with their own sets of material parameters. To determine these parameters for one steel grade each phenomenon has to be investigated experimentally under a wide range of process conditions. However, steel companies for example produce a wide range of different steel grades, so there is a great interest in reducing the required experimental work. In particular the determination of the grain size is difficult since the prior austenite grain boundaries cannot easily be revealed with metallographic techniques for a lot of modern low carbon steels.

Another motivation for the usage of less phenomenological but more physical based models is to increase the predictive capabilities. Numerical simulation of an industrial hot rolling process using models developed on the basis of laboratory tests are in most cases extrapolations of the underlying experimental data. In a typical hot rolling process strain rates up to $150 \frac{1}{s}$ and overall strains up to $\varepsilon = 5$ are possible. These conditions are difficult to simulate experimentally on a laboratory scale. During multistage deformation recrystallization may not always be completed. The microstructure can consist of multiple generations of grains that have been recrystallized at different points of time. This can not be modeled adequately when only considering average values of the grain size and the recrystallized volume fraction.

Mesoscale models that use a spatial representation of the microstructure give an opportunity to simulate the physical processes involved in recrystallization during hot rolling. In particular models based on the Cellular Automata method show promising results like the simulation of *DRX* under transient conditions by Kroc [33] that show similar patterns as the experimental results from Frommert [9] and Sakai et al. [1]. The simulation results of post-deformation recrystallization by Kugler and Turk [41] show that *MDRX* and *SRX* can be described with one unified model. This can be explained by the influence of the current grain size on the recrystallization kinetics. The size of the grains recrystallized by *DRX* depends on strain rate and temperature. Hence the kinetics of *MDRX* also depends on strain rate and temperature of the previous deformation. However the initial grain size for *SRX* does not change due to the deformation condition because in this case no *DRX* is involved. So *SRX* depends more on temperature and the grain size prior to deformation than on strain rate. Other benefits of such models are, that the virtual microstructure can easily be compared

with a real microstructure. It is also possible to track multiple generation of recrystallized grains. However, the *CA* method is very computationally and memory intensive, especially if a three-dimensional lattice is used. It is therefore not suited yet for a direct usage in forming simulations or process control applications.

The proposed ensemble model describes each grain with a set of scalar variables. Compared to *CA* models this reduces the required amount of memory and computation cycles proportional to the number of cells needed to describe one grain in a *CA* lattice. A spherical grain with a grain diameter of $20 \mu\text{m}$ fills approximately 4200 cells in a three-dimensional lattice with an edge length of $2 \mu\text{m}$ of each cell. The trade off is that the model only provides the distribution of the grain size rather than a spatial representation of the microstructure. The model holds no information about the relationship between the grains. It is not possible to take into account the difference of the misorientation between the grains for the calculations of the grain boundary energy, so an average value is used. But like in vertex models the grains are not discretized so grain boundary movement can be described continuously. Similar to *CA* models the ensemble model can describe the transient oscillation that can be observed at transient conditions during deformation. The system does not change its state instantly to the configuration with the lowest free energy. Instead, work has to be performed to move the grain boundaries. This is a time dependent and dissipative process that follows the principle of least actions. The path with the lowest energy dissipation is in some cases an oscillation of the average grain size and the flow stress.

6. Conclusion

Mesoscale models allow the modeling of the microstructure evolution during and after hot deformation by describing the underlying physical processes. Phenomena modeled separately by constitutive models like *DRX*, *SRX*, *MDRX* and grain growth can be described in a unified manner. The outlined ensemble model makes some approaches known from mesoscale models practically useable for through process modeling and process control application by a massive reduction of the required computational effort.

All models rely on proper material parameters. Future work should therefore focus on methods for the determination of model parameters, especially for the models based on physical approaches. One way to determine the parameters from experimental data is the use of the inverse analysis method. This implies the execution of many simulation cycles that are time consuming for complex models. The usage of the ensemble model can be a solution to make such analysis feasible.

Models for recrystallization

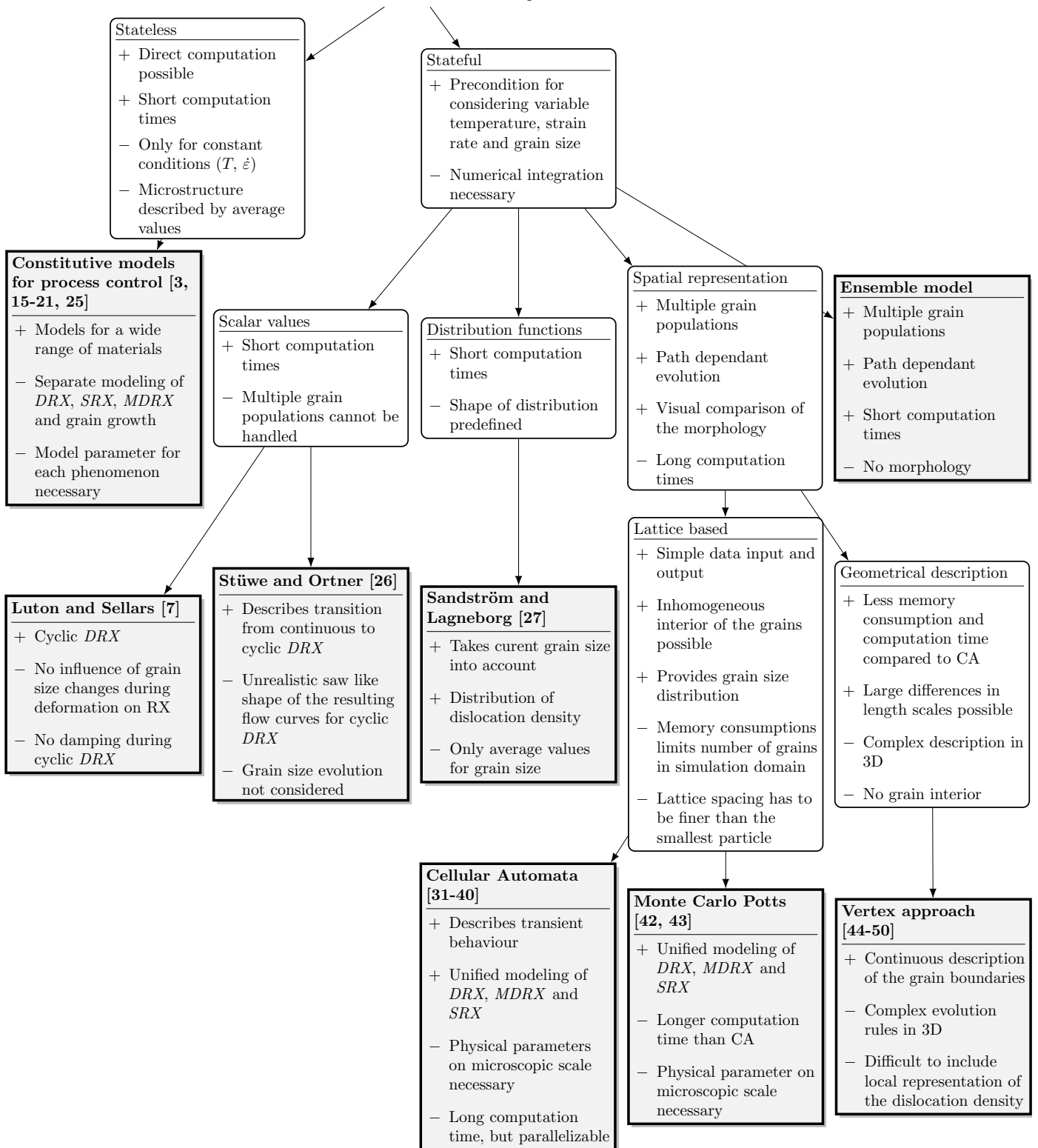


Figure 7: Hierarchical overview of the features and constraints of different model approaches for recrystallization. The models (highlighted with a thick border) are divided in several branches based on the underlying modeling techniques.

References

- [1] T. Sakai, A. Belyakov, R. Kaibyshev, H. Miura, J. J. Jonas, Dynamic and post-dynamic recrystallization under hot, cold and severe plastic deformation conditions, *Prog. Mater. Sci.* 60 (2014) 130–207, ISSN 0079-6425, doi:10.1016/j.pmatsci.2013.09.002.
- [2] J. N. Greenwood, H. K. Wornor, Types of creep curve obtained with lead and its dilute alloys, *Journal Institute of Metals* 64 (1939) 135.
- [3] T. Senuma, M. Suehiro, H. Yada, Mathematical models for predicting microstructural evolution and mechanical properties of hot strips, *ISIJ Int.* 32 (3) (1992) 423–432.
- [4] M. Militzer, Computer simulation of microstructure evolution in low carbon sheet steels, *ISIJ international* 47 (1) (2007) 1–15.
- [5] H. Hallberg, Approaches to modeling of recrystallization, *Metals* 1 (1) (2011) 16–48.
- [6] N. Xiao, Y. Chen, D. Li, Y. Li, Progress in mesoscopic modeling of microstructure evolution in steels, *Sci. China Technol. Sci.* 55 (2) (2012) 341–356, ISSN 1674-7321, 1869-1900, doi:10.1007/s11431-011-4699-z.
- [7] M. Luton, C. Sellars, Dynamic recrystallization in nickel and nickel-iron alloys during high temperature deformation, *Acta Metall.* 17 (8) (1969) 1033–1043, ISSN 0001-6160, doi:10.1016/0001-6160(69)90049-2, 00398.
- [8] T. Sakai, J. J. Jonas, Overview no. 35 Dynamic recrystallization: Mechanical and microstructural considerations, *Acta Metall.* 32 (2) (1984) 189–209.
- [9] M. M. Frommert, *Dynamische Rekristallisation unter konstanten und transienten Umformbedingungen*, Cuvillier Verlag, ISBN 9783867274968, 00001, 2008.
- [10] M. Frommert, G. Gottstein, Mechanical behavior and microstructure evolution during steady-state dynamic recrystallization in the austenitic steel 800H, *Mater. Sci. Eng., A* 506 (1–2) (2009) 101–110, ISSN 0921-5093, doi:10.1016/j.msea.2008.11.035.
- [11] C. Sellars, J. Whiteman, Recrystallization and grain growth in hot rolling, *Met. Sci.* 3 (4) (1979) 187–194.
- [12] Q. Wang, J. Lai, D. L. Sun, Artificial neural network models for predicting flow stress and microstructure evolution of a hydrogenized titanium alloy, *Key Eng. Mater.* 353-358 (2007) 541–544, ISSN 1662-9795, doi:10.4028/www.scientific.net/KEM.353-358.541.
- [13] M. P. Phaniraj, A. K. Lahiri, The applicability of neural network model to predict flow stress for carbon steels, *J. Mater. Process. Technol.* 141 (2) (2003) 219–227, ISSN 0924-0136, doi:10.1016/S0924-0136(02)01123-8.
- [14] S. Mandal, P. V. Sivaprasad, R. K. Dube, Modeling microstructural evolution during dynamic recrystallization of alloy D9 using artificial neural network, *J. Mater. Eng. Perform.* 16 (6) (2007) 672–679, ISSN 1059-9495, 1544-1024, doi:10.1007/s11665-007-9098-z.
- [15] M. Ji, R. Shivpuri, Reduction of random seams in hot rolling through FEM based sensitivity analysis, *Mater. Sci. Eng., A* 425 (1–2) (2006) 156–166, ISSN 0921-5093, doi:10.1016/j.msea.2006.03.071.
- [16] G. R. Gómez, T. Pérez, Modelling the microstructural evolution during hot rolling, *Latin American applied research* 32 (3) (2002) 253–256.
- [17] M. Gómez, L. Rancel, B. J. Fernández, S. F. Medina, Evolution of austenite static recrystallization and grain size during hot rolling of a V-microalloyed steel, *Mater. Sci. Eng., A* 501 (1–2) (2009) 188–196, ISSN 0921-5093, doi:10.1016/j.msea.2008.09.074.
- [18] W. Sun, E. Hawbolt, Comparison between static and metadynamic recrystallization—an application to the hot rolling of steels, *ISIJ Int.* 37 (10) (1997) 1000–1009.
- [19] S. Davenport, N. Silk, C. Sparks, C. Sellars, Development of constitutive equations for modelling of hot rolling, *Mater. Sci. Technol.* 16 (2000) 539–546.
- [20] P. Uranga, A. Fernández, B. López, J. Rodríguez-Ibabe, Transition between static and metadynamic recrystallization kinetics in coarse Nb microalloyed austenite, *Materials Science and Engineering: A* 345 (1–2) (2003) 319–327, ISSN 0921-5093, doi:10.1016/S0921-5093(02)00510-5, 00070.
- [21] S.-I. Kim, Y. Lee, D.-L. Lee, Y.-C. Yoo, Modeling of AGS and recrystallized fraction of microalloyed medium carbon steel during hot deformation, *Mater. Sci. Eng., A* 355 (1–2) (2003) 384–393, ISSN 0921-5093, doi:10.1016/S0921-5093(03)00104-7.
- [22] C. Zener, J. Hollomon, Effect of strain rate upon plastic flow of steel, *J. Appl. Phys.* 15 (1944) 22, 00000.
- [23] G. Kugler, M. Knap, H. Palkowski, R. Turk, Estimation of activation energy or Calculating the hot workability properties of metals, *Metalurgija* 43 (4) (2004) 267–272.
- [24] M. Avrami, Kinetics of phase change. I General theory, *J. Chem. Phys.* 7 (1939) 1103.
- [25] P. D. Hodgson, R. K. Gibbs, A Mathematical model to predict the mechanical properties of hot rolled C-Mn and microalloyed steels, *ISIJ Int.* 32 (12) (1992) 1329–1338, ISSN 0915-1559, doi:10.2355/isijinternational.32.1329.
- [26] H. P. Stüwe, B. Ortner, Recrystallization in hot working and creep, *Met. Sci.* 8 (1) (1974) 161–167.
- [27] R. Sandström, R. Lagneborg, A model for hot working occurring by recrystallization, *Acta Metall.* 23 (3) (1975) 387–398, ISSN 0001-6160, doi:10.1016/0001-6160(75)90132-7.
- [28] R. Sandström, R. Lagneborg, A model for hot working occurring by recrystallization, *Scripta Metallurgica* 8 (11) (1974) liv–lv, ISSN 0036-9748, doi:10.1016/0036-9748(74)90362-7.
- [29] S. M. Ulam, *Adventures of a Mathematician*, University of California Press, ISBN 9780520910553, 1991.
- [30] J. Von Neumann, The general and logical theory of automata, *Cerebral mechanisms in behavior* (1951) 1–41.
- [31] H. Hesselbarth, I. Göbel, Simulation of recrystallization by cellular automata, *Acta Mater. et Metall.* 39 (9) (1991) 2135–2143, ISSN 0956-7151, doi:10.1016/0956-7151(91)90183-2.
- [32] R. Ding, Z. X. Guo, Coupled quantitative simulation of microstructural evolution and plastic flow during dynamic recrystallization, *Acta materialia* 49 (16) (2001) 3163–3175.
- [33] J. Kroc, Application of cellular automata simulations to modelling of dynamic recrystallization, in: P. M. A. Sloom, A. G. Hoekstra, C. J. K. Tan, J. J. Dongarra (Eds.), *Computational Science — ICCS 2002*, no. 2329 in *Lecture Notes in Computer Science*, Springer Berlin Heidelberg, ISBN 978-3-540-43591-4, 978-3-540-46043-5, 773–782, 2002.
- [34] D. Kuc, J. Gawad, Modelling of microstructure changes in hot deformed materials using cellular automata, *AIP Conf. Proc.* 1315 (1) (2011) 1479–1484, doi:10.1063/1.3552396.
- [35] G. Kugler, R. Turk, Study of the influence of initial microstructure topology on the kinetics of static recrystallization using a cellular automata model, *Comp. Mater. Sci.* 37 (3) (2006) 284–291, ISSN 0927-0256, doi:10.1016/j.commatsci.2005.07.005.
- [36] H. W. Lee, Y.-T. Im, Cellular automata modeling of grain coarsening and refinement during the dynamic recrystallization of pure copper, *Materials Transactions* 51 (9) (2010) 1614.
- [37] M. Qian, Z. X. Guo, Cellular automata simulation of microstructural evolution during dynamic recrystallization of an HY-100 steel, *Mater. Sci. Eng., A* 365 (1-2) (2004) 180–185, ISSN 0921-5093, doi:10.1016/j.msea.2003.09.025.
- [38] H. Won Lee, Y.-T. Im, Numerical modeling of dynamic recrystallization during nonisothermal hot compression by cellular automata and finite element analysis, *Int. J. Mech. Sci.* 52 (10) (2010) 1277–1289, ISSN 0020-7403, doi:10.1016/j.ijmecsci.2010.06.003.
- [39] N. Yazdipour, C. Davies, P. Hodgson, Microstructural modeling of dynamic recrystallization using irregular cellular automata, *Comp. Mater. Sci.* 44 (2) (2008) 566–576, ISSN 0927-0256, doi:10.1016/j.commatsci.2008.04.027.
- [40] Y. Liu, T. Baudin, R. Penelle, Simulation of normal grain growth by cellular automata, *Scripta Mater.* 34 (11).
- [41] G. Kugler, R. Turk, Modeling the dynamic recrystallization under multi-stage hot deformation, *Acta Materialia* 52 (15) (2004) 4659–4668, ISSN 1359-6454, doi:10.1016/j.actamat.2004.06.022.
- [42] P. S. Sahni, D. J. Srolovitz, G. S. Grest, M. P. Anderson, S. A. Safran, Kinetics of ordering in two dimensions. II. Quenched systems, *Phys. Rev. B* 28 (5) (1983) 2705–2716, doi:10.1103/PhysRevB.28.2705.
- [43] D. Zöllner, P. Streitenberger, Computer simulations and statistical theory of normal grain growth in two and three dimensions, *Mater. Sci. Forum* 467-470 (2004) 1129–1136, ISSN 1662-9752, doi:10.4028/www.scientific.net/MSF.467-470.1129.
- [44] A. Cocks, S. Gill, A variational approach to two dimensional grain growth—I. Theory, *Acta Mater.* 44 (12) (1996) 4765–4775, ISSN 1359-6454, doi:10.1016/S1359-6454(96)00121-8.
- [45] D. Weygand, J. Lépinoux, Y. Bréchet, On the Nucleation of Abnormal Grain Growth: A 2D Vertex Simulation, *Mater. Sci. Forum* 467-470 (2004) 1123–1128, ISSN 1662-9752, doi:10.4028/www.scientific.net/MSF.467-470.1123, 00000.
- [46] S. Lloyd, Least squares quantization in PCM, *Information Theory, IEEE*

- Transactions on 28 (2) (1982) 129–137.
- [47] T. Nagai, S. Ohta, K. Kawasaki, T. Okuzono, Computer simulation of cellular pattern growth in two and three dimensions, *Phase Transitions* 28 (1-4) (1990) 177–211, ISSN 0141-1594, doi:10.1080/01411599008207938.
- [48] S. Gill, A. Cocks, A variational approach to two dimensional grain growth—II. Numerical results, *Acta Mater.* 44 (12) (1996) 4777–4789, ISSN 1359-6454, doi:10.1016/S1359-6454(96)00122-X.
- [49] H. Telley, T. M. Liebling, A. Mocellin, The Laguerre model of grain growth in two dimensions I. Cellular structures viewed as dynamical Laguerre tessellations, *Philos. Mag. B* 73 (3) (1996) 395–408, ISSN 1364-2812, doi:10.1080/13642819608239125.
- [50] E. Schüle, A justification of the Hillert distribution by spatial grain growth simulation performed by modifications of Laguerre tessellations, *Comp. Mater. Sci.* 5 (4) (1996) 277–285, ISSN 0927-0256, doi:10.1016/0927-0256(96)00004-3.